MCB
Journals.ASM.org

The Tumor Necrosis Factor Receptor Stalk Regions Define Responsiveness to Soluble versus Membrane-Bound Ligand

Christine Richter,[a]* Sylvia Messerschmidt,[b] Gerlinde Holeiter,[b] Jessica Tepperink,[b] Sylvia Osswald,[b] Andrea Zappe,[c] Marcus Branschädel,[b] Verena Boschert,[b] Derek A. Mann,[d] Peter Scheurich,[b] and Anja Krippner-Heidenreich[a]

Institute of Cellular Medicine, Musculoskeletal Research Group,[a] and Liver Research Group,[d] Newcastle University, Newcastle upon Tyne, United Kingdom, and Institute of Cell Biology and Immunology[b] and Institute of Physics and Research Center SCoPE,[c] University of Stuttgart, Stuttgart, Germany

The family of tumor necrosis factor receptors (TNFRs) and their ligands form a regulatory signaling network that controls immune responses. Various members of this receptor family respond differently to the soluble and membrane-bound forms of their respective ligands. However, the determining factors and underlying molecular mechanisms of this diversity are not yet understood. Using an established system of chimeric TNFRs and novel ligand variants mimicking the bioactivity of membrane-bound TNF (mTNF), we demonstrate that the membrane-proximal extracellular stalk regions of TNFR1 and TNFR2 are crucial in controlling responsiveness to soluble TNF (sTNF). We show that the stalk region of TNFR2, in contrast to the corresponding part of TNFR1, efficiently inhibits both the receptor's enrichment/clustering in particular cell membrane regions and ligand-independent homotypic receptor preassembly, thereby preventing sTNF-induced, but not mTNF-induced, signaling. Thus, the stalk regions of the two TNFRs not only have implications for additional TNFR family members, but also provide potential targets for therapeutic intervention.

Tumor necrosis factor (TNF) is a central proinflammatory regulator of the innate immune system mainly produced by macrophages and other cells of the immune system (41). TNF is an important modulator of cell function and is critically involved in immune homeostasis, carcinogenesis, and stem cell development (41, 56, 62). The cytokine is also associated with the pathophysiology of several acute and chronic diseases, including neurodegenerative, fibrotic, and autoimmune diseases. Neutralization of TNF in autoimmune diseases, such as rheumatoid arthritis, inflammatory bowel disease, and psoriasis, represents a major therapeutic success story, illustrating the importance of the cytokine in disease progression (70). However, the use of TNF-specific drugs leads to heterogeneous clinical responses and, in some cases, undesirable side effects, such as infection, autoimmune exacerbations, increased risk of congestive heart failure, and lymphomas (78). These effects highlight the complexity of TNF signaling.

TNF is produced as a typical type II transmembrane protein (membrane-bound TNF [mTNF]), which can be cleaved by metalloproteases to release the soluble ligand (sTNF) (77). Evidence for distinct roles of mTNF and sTNF *in vivo* has been obtained from diverse studies of genetically modified mice. These animal models demonstrate that sTNF is required for the development of acute and chronic inflammation, whereas mTNF supports processes underlying the development of lymphoid tissue and protection against intracellular bacterial infections, chronic inflammation, and autoimmunity (2, 36, 64–66). For example, mTNF exerts autoimmune-suppressive functions in the autoimmune encephalomyelitis model of demyelination (EAE model) and was insufficient to support the development of chronic arthritis. In contrast, wild-type TNF promoted inflammation in the EAE model and arthritogenic functions in diverse mouse models of arthritis (1, 3). In general, it seems that mTNF has distinct beneficial functions while lacking sTNF's harmful ones. This may explain its apparently contradictory observed effects, such as its pro- versus anti-inflammatory activities or growth stimulation versus apoptosis induction (41).

Cellular TNF responses are mediated through signaling via two members of the TNF receptor (TNFR) superfamily, TNFR1 (CD120a) and TNFR2 (CD120b) (41). Whereas TNFR1 is ubiquitously expressed at low levels with a few hundred binding sites per cell, TNFR2 expression is highly regulated and is primarily found on cells of the immune system, but also on endothelial and neurological tissues. Differential responsiveness of the two TNFRs to sTNF provides an important layer of complexity in the regulation of TNF responses. Whereas TNFR1 can be fully activated by both forms of TNF, TNFR2 is efficiently activated only by mTNF, despite binding sTNF with high affinity (24). Thus, mTNF-mediated signaling occurs in a juxtacrine fashion through cell-cell contacts, whereas sTNF is capable of promoting paracrine and systemic functions via TNFR1. The reason for these differential activation patterns, which are also exhibited by other TNF superfamily members, is unclear at present, but we have previously shown that the regulatory mechanism for the TNFR system is located upstream of receptor-signaling complex formation (38) and was proposed to be linked to the association/dissociation kinetics of the given ligand-receptor pair (25).

Once activated, both TNFRs use distinct, but partly overlapping, signaling pathways. TNFR1 initiates strong NF-κB signaling and efficient activation of caspases via its cytoplasmic death do-

Received 21 October 2011 **Returned for modification** 15 November 2011
Accepted 18 April 2012

Published ahead of print 30 April 2012

Address correspondence to Anja Krippner-Heidenreich, anja.krippner-heidenreich@ncl.ac.uk.

* Present address: Division of Molecular Structure, MRC-National Institute for Medical Research London, United Kingdom.

Supplemental material for this article may be found at http://mcb.asm.org/.

doi:10.1128/MCB.06458-11

main. It is also capable of initiating necrotic and necroptotic signaling, finally leading to cell death (50). In contrast, TNFR2, which lacks a death domain, initiates cytoprotective functions through both classical and nonclassical NF-κB pathways (50, 61). Hence, TNFR1 and TNFR2 are capable of transmitting opposing signals (6, 22, 41, 54), with TNFR2 being capable of suppressing TNFR1-mediated proinflammatory responses and exerting neuroprotective and tissue regeneration functions in animal models of diverse pathologies (3, 6, 50, 51, 54). TNFR1-independent functions of TNFR2 have been convincingly demonstrated in T cells, showing the importance of TNFR2 for antigen-stimulated activation, proliferation, and survival (25, 31–33). More recently, a role for TNFR2 signaling in the selective killing of autoreactive T cells (4) and the promotion of regulatory T-cell function and expansion (14) have been demonstrated. In line with this, tolerogenic roles of mTNF could also be attributed to TNFR2 (1, 34). Indeed, the importance of differential signaling via TNFR1 and TNFR2 in balancing specific immune responses provides a potential target to improve anti-TNF therapies (11, 14, 20, 36) and requires a more detailed understanding of the differential responsiveness of the two TNFRs to sTNF.

Here, we made use of our previously developed unique cellular system comprising human TNFR chimeras expressed in cells lacking TNFR background and novel TNF variants mimicking mTNF bioactivity (10, 38). The chimeras contain the relevant TNFR extracellular domain fused to the intracellular domain of Fas (TNFR-Fas). They allow exogenous expression of the otherwise cytotoxic TNFR1 and, in addition, link the signaling of the two TNFR molecules to identical pathways while maintaining the different patterns of response to sTNF. By swapping various domains between TNFR1 and TNFR2, as well as investigating specific receptor variants, we identified a particular extracellular region proximal to the transmembrane region, referred to as the "stalk region," which effectively prevents sTNF responsiveness via TNFR2. We demonstrate that a fundamental parameter determining the responsiveness of TNFRs to sTNF is their arrangement in the plasma membrane in the absence of ligand. Ligand-independent local enrichment of receptors confers sTNF responsiveness and perfectly correlates with enhanced pre-ligand binding assembly domain (PLAD)-mediated homomultimer formation. Due to a high degree of homology within the TNFR superfamily, our results are likely to be relevant to other members. In the long run, the stalk regions of TNFR family members could represent potential targets for the modulation of cellular responses, for example, by enhancing selective killing of autoreactive T cells and/or promoting regulatory T-cell functions in autoimmune diseases.

MATERIALS AND METHODS

A detailed description of molecular cloning can be found in the supplemental material.

Cell culture, antibodies, and reagents. Simian virus 40 large-T-immortalized murine embryonic fibroblasts (MF) from *tnfr1*$^{-/-}$ *tnfr2*$^{-/-}$ double-knockout mice were kindly supplied by Daniela Männel (University of Regensburg, Regensburg, Germany). HeLa cells were obtained from ATCC and HEK 293 Flp-In T-Rex cells from Invitrogen. MF, HeLa cells, and cell lines derived from them were cultivated in RPMI 1640 supplemented with 5% (vol/vol) fetal calf serum (FCS) and 2 mM L-glutamine. KYM-1 cells were cultured in RPMI 1640 supplemented with 2 mM L-glutamine and 10% (vol/vol) fetal calf serum. Stably transfected HEK 293 Flp-In T-Rex cells were grown in Dulbecco's modified Eagle's medium (DMEM), 4.5 g/liter glucose, L-glutamine medium supplemented with 10% (vol/vol) FCS, 15 μg/ml blasticidin S, and 100 μg/ml hygromycin B (both from Invitrogen Ltd.). Recombinant human TNF (2×10^7 units/mg) was provided by Knoll AG (Ludwigshaven, Germany). The cloning, expression, and purification of recombinant CysTNF, a TNF mutant carrying a cysteine residue near the N terminus, were performed as described previously (10). Briefly, His-tagged CysTNF was purified with the help of a nickel column, and endotoxin was removed with EndoTrap (Profos AG). The various antibodies were obtained as follows: mouse anti-human TNFR1 IgG2a (H398) and mouse anti-human TNFR2 IgG1 (MR2-1) were from Hbt Hycult; anti-active caspase 3 IgG (C92-605) and mouse anti-human TRAF2 IgG2a (C90-481) were from BD; Fas-specific antibodies (B10) and rabbit anti-human p65 IgG (C-20/sc-372) were from Santa Cruz; fluorescein isothiocyanate (FITC)-conjugated goat anti-mouse IgG plus IgM and goat anti-mouse IgG-horseradish peroxidase (HRP) were from Dianova; goat anti-human TNFR2 was from R&D; and Alexa Fluor 594-conjugated goat anti-rabbit IgG was from Invitrogen. The rabbit serum was obtained from Sigma, bis-(sulfosuccinimidyl)-suberate (BS^3) was purchased from Perbio, the protease inhibitors from Roche Applied Science, and z-Val-Ala-DL-Asp-fluoromethylketone (zVAD-fmk) from Bachem.

Generation of stable cell lines and transient protein expression. MF stably transfected with chimeric receptors consisting of the intracellular portion of Fas and the extracellular and transmembrane regions of TNFR1 (TNFR1-Fas) and TNFR2 (TNFR2-Fas), respectively, were generated and described previously (38). All other receptor constructs were stably transfected into MF using Lipofectamine 2000 (Invitrogen Ltd.) and a protocol detailed previously (38). For the generation of HeLa cells stably expressing wild-type TNFR2 and variants thereof, 2.5×10^5 cells/well were seeded into 6-well plates, grown overnight, and transfected using Effectene (Qiagen). The next day, cells were selected with 3 μg/ml puromycin A. The medium was replaced every 2 to 3 days, and 2 weeks later, they were sorted for TNFR2- and TNFR2 variant-positive cells by flow cytometry using FACSDiva (Becton Dickinson) as described previously (38). Doxycyline-inducible HEK 293 Flp-In T-Rex cells expressing TNFR1-Fas were generated previously (9). HEK 293 Flp-In T-Rex cells inducibly expressing TNFR1-S2T2-Fas, TNFR1-$S2_{\Delta 42}$T2-Fas, TNFR2-Fas, TNFR2-S1T1-Fas, TNFR2-$S2_{\Delta 42}$T2-Fas, wild-type TNFR2, TNFR2-S1T1-R2, and TNFR2-$S2_{\Delta 42}$T2-R2 were generated by stable transfection of pcDNA/FRT/TO encoding the respective construct. The cells were grown in T75 cell culture flasks to 75% confluence and transfected with the pcDNA/FRT/TO vector encoding the receptor and the Flp recombinase-encoding pOG44 vector in a 1:10 ratio using the TransIt-293 system (Mirus Bio). Two days after transfection, cells were selected with 15 μg/ml blasticidin S and 100 μg/ml hygromycin B. The medium was replaced every 4 to 5 days, and a typical cell line was obtained from 5 to 10 isogenic clones.

For transient transfections of HeLa cells with expression constructs in which O-glycosylation sites had been mutated, 2.5×10^5 cells/well were seeded into 6-well plates, grown overnight, transfected using Effectene (Qiagen), and harvested the next day.

Cell viability and apoptosis assays. Cell viability assays with MF stably expressing TNFR-Fas chimeras were performed as described previously (38). Briefly, 1×10^4 cells/well were seeded into 96-well plates and grown overnight. The next day, the cells were stimulated for 8 h as indicated and then stained with crystal violet solution (0.5% [wt/vol] crystal violet, 20% [vol/vol] methanol) for 15 min. The plates were washed with H_2O and air dried. The dye was resolved in methanol, and the optical density at 550 nm was measured on a microplate reader (Sunrise; Tecan Ltd.). The 50% effective dose (ED_{50}) of the diverse ligands and the indicated standard error of the mean (SEM) were determined by using GraphPad Prism software. For the analysis of active caspase 3 levels, HEK 293 Flp-In T-Rex cells expressing various TNFR-Fas and TNFR2 variants (2×10^5 cells) were induced with 6 ng/ml of doxycycline for 18 h or left untreated. Cells were harvested, fixed with Cytofix/Cytoperm buffer (BD), washed with Wash/Perm buffer (BD), and incubated with

Wash/Perm buffer containing 2% (vol/vol) rabbit serum for 15 min on ice. Phycoerythrin (PE)-conjugated rabbit anti-active caspase 3 antibodies (1:13) were added, and the cells were stained at room temperature for 20 min. The cells were washed with Wash/Perm buffer, resuspended in PBA (0.25% [wt/vol] bovine serum albumin [BSA], 0.02% [wt/vol] NaN_3 in phosphate-buffered saline [PBS]) and acquired on a FACSCanto II flow cytometer.

Coimmunoprecipitation of TNFR2-TRAF2 complexes. HeLa cells stably expressing wild-type TNFR2 and variants thereof (2.5×10^5 cells/well) were seeded into 6-well plates. The next day, cells were left untreated or were treated with sTNF or CysTNF (10 ng/ml each) for 5 to 15 min at 37°C. The cells were washed with ice-cold PBS, harvested, and pelleted. The cells were then lysed in solubilization buffer (20 mM Tris-HCl, pH 7.5, 150 mM NaCl, 1 mM EDTA, 1% [vol/vol] Triton X-100, 30 mM NaF) supplemented with protease inhibitors and 0.5 mM phenylmethylsulfonyl fluoride (PMSF). Two micrograms of monoclonal goat anti-human soluble TNFR2 antibodies was added and incubated at 4°C for 2 h prior to the addition of 10 μl of protein G Sepharose beads (Invitrogen) for 1 h on a rotary mixer at 4°C. The beads were washed with solubilization buffer, and Laemmli sample buffer with 5% (vol/vol) 2-mercaptoethanol was added.

Western blot analyses. Protein samples were supplemented with Laemmli buffer containing 5% 2-mercaptoethanol, resolved by SDS-PAGE, and then transferred to nitrocellulose membranes. TNFR-Fas chimeras were detected using anti-Fas antibodies and TRAF2 was detected by anti-human TRAF2 antibodies, in combination with either goat anti-mouse IgG-HRP or goat anti-rabbit IgG-HRP antibodies. SuperSignal West Pico or SuperSignal West Dura chemiluminescence substrate (Thermo Scientific/Pierce) was used, and chemiluminescence was captured on Kodak BioMax MR autoradiography films (Sigma-Aldrich) or detected using a Syngene G:Box and GeneSnap v7.09 acquisition software (Syngene). Western blot band quantification was performed using GeneTools v4.01 analysis software (Syngene).

Microscopy analyses. For the analysis of nuclear translocation of p65, 5×10^4 MF expressing wild-type TNFR2 and variants thereof were seeded onto glass coverslips in a 24-well plate. The next day, the cells were stimulated with sTNF or CysTNF (100 ng/ml each) for 30 min at 37°C. The cells were washed with ice-cold PBS and fixed with 3.7% formaldehyde for 10 min at room temperature. The cells were then washed with PBS, permeabilized with saponin solution (0.1% [wt/vol] saponin, 0.5% [wt/vol] BSA in PBS) for 10 min, and blocked with 3% (wt/vol) BSA in PBS for 45 min. Coverslips were stained with rabbit anti-human p65 IgG (1:100) for 2 h, washed with PBS, and stained with Alexa Fluor 594-conjugated goat anti-rabbit IgG (1:100) for 1 h. The coverslips were washed with PBS and mounted on microscope slides using Vectashield DAPI (4′,6-diamidino-2-phenylindole)-containing mounting medium. Images were acquired at ×40 magnification on a Zeiss Axio Imager 2 fluorescence microscope using AxioVision 4.7.2 software. For quantifications of nuclear p65 levels, more than 200 cells were microscopically assessed. The mean percentage and standard deviation were calculated from three independent experiments. For receptor cell surface distribution analysis, 8×10^4 HEK Flp-In T-Rex cells/well were seeded onto poly-L-lysine-coated glass coverslips in 12-well plates and grown for 6 h. The cells were left untreated or induced with 6 ng/ml doxycycline for 18 h, in the case of cell lines inducibly overexpressing TNFR-Fas chimeras, in combination with 10 μM zVAD-fmk when not otherwise stated. sTNF was labeled using the Alexa Fluor 546 Protein Labeling Kit (Molecular Probes Inc.) according to the manufacturer's instructions. Briefly, sTNF (1 mg/500 μl) was mixed with 50 μl 1 M bicarbonate buffer and the reactive dye and incubated for 1 h at room temperature. sTNF-Alexa Fluor 546 was purified by exclusion gel chromatography, and the bioactivity was verified in cytotoxicity assays. The cells were washed with ice-cold PBS, stained with 1.7 μg/ml Alexa Fluor 546-labeled sTNF on ice for 5 min, washed again with ice-cold PBS, and fixed with 4% formaldehyde at room temperature for 20 min. The coverslips were washed and mounted on glass microscope slides using Fluoromount G mounting medium (Southern Biotech). Images were acquired on an Andor Revolution XD confocal microscope using Andor iQ 1.9.1 software. For quantitative analyses, images closest to the glass surface were cropped to generate images with definable cell counts, and receptor clusters were analyzed using Volocity (PerkinElmer) image analysis software. The images were subjected to thresholding using a standard deviation of 1.5 above the mean pixel intensity of the region selected. Receptor clusters ranging from 0.04 to 9.72 μm^2 were quantified and expressed as the average number of clusters per cell.

TNF dissociation kinetics experiments. TNF was labeled with ^{125}I using the chloramine-T method, and bioactivity was determined via cell viability assays on KYM-1 cells. The dissociation kinetics experiments were performed as described previously (25). Cells were incubated in binding buffer with ^{125}I-labeled TNF (60 ng/ml) for 1 h on ice in the absence or presence of a 200-fold excess of unlabeled TNF. Fifty microliters of cell suspension was suspended in 100 μl of prewarmed binding buffer (37°C) containing a 150-fold excess of unlabeled TNF on a layer of phthalate oil and immediately centrifuged or incubated for different times (10 s to 10 min) prior to centrifugation. Cell-bound radioactivity after centrifugation was determined as described previously (25).

Immunostaining and flow cytometry. For cell surface staining of TNFR2, TNFR1-Fas, TNFR2-Fas, and variants thereof, 5×10^5 cells were harvested and resuspended in PBA containing 5 μg/ml mouse anti-human TNFR1 and 2.5 μg/ml mouse anti-human TNFR2 and incubated on ice for 1 h. The cells were washed with PBA and incubated with FITC-conjugated goat anti-mouse IgG plus IgM antibodies in PBA for 1 h on ice prior to analysis by flow cytometry on a FACSCanto II (Becton Dickinson) or an Epics XL-MCL (Beckman Coulter). The percentages of cells that gated positive and the median fluorescence intensities (MnX) were calculated using FlowJo analysis software.

Chemical protein cross-linking of TNFR-Fas chimeras. Chemical protein cross-linking of TNFR-Fas chimeras was performed as described previously (9). MF TNFR-Fas variants were seeded into 6-well plates (3×10^5 cells/well). The next day, the cells were washed with ice-cold PBS and left untreated or incubated with increasing concentrations of the NH_2-reactive cross-linking reagent BS^3 (33 μM to 500 μM) for 30 min on ice. The reaction was stopped by addition of 10 mM Tris-HCl, pH 7.2, and incubation at room temperature for 15 min. Cells were harvested, pelleted, and lysed in buffer A (20 mM Tris-HCl, pH 7.5, 150 mM NaCl, 1 mM EDTA, 1% [vol/vol] TritonX-100) supplemented with protease inhibitors. Protein loading was corrected for equal protein content using BradfordUltra reagent (Expedeon) and receptor cell surface expression as determined by flow cytometry.

RESULTS

The stalk regions of TNFR1 and TNFR2 control sTNF responsiveness. To elucidate the molecular determinant(s) of the different responsiveness of TNFR1 and TNFR2 to sTNF, we swapped and deleted different regions between the two TNFRs (Fig. 1). These receptor variants were stably expressed as TNFR-Fas chimeras in fibroblasts (MF) from *tnfr1*$^{-/-}$ *tnfr2*$^{-/-}$ double-knockout mice, and the response patterns were compared in standardized cytotoxicity assays. TNFR1 and TNFR2 are both readily activated by mTNF. Accordingly, the efficient activation of the various TNFR-Fas chimeras by CysTNF, an oligomerized TNF derivative featuring mTNF-like bioactivity (10, 38), and CHOΔ1-12TNF (CHO cells expressing a mutant form of membrane-bound TNF that cannot be processed to sTNF), but not wild-type CHO cells, indicated that all receptor variants were comparably signaling competent (ED_{50} = 0.1 to 0.3 ng/ml) (Fig. 2; see Fig. S2 in the supplemental material). MF expressing TNFR1-Fas readily underwent apoptosis after stimulation with increasing concentrations of sTNF (ED_{50} = 0.1 ng/ml) (Fig. 2A) (38). In contrast,

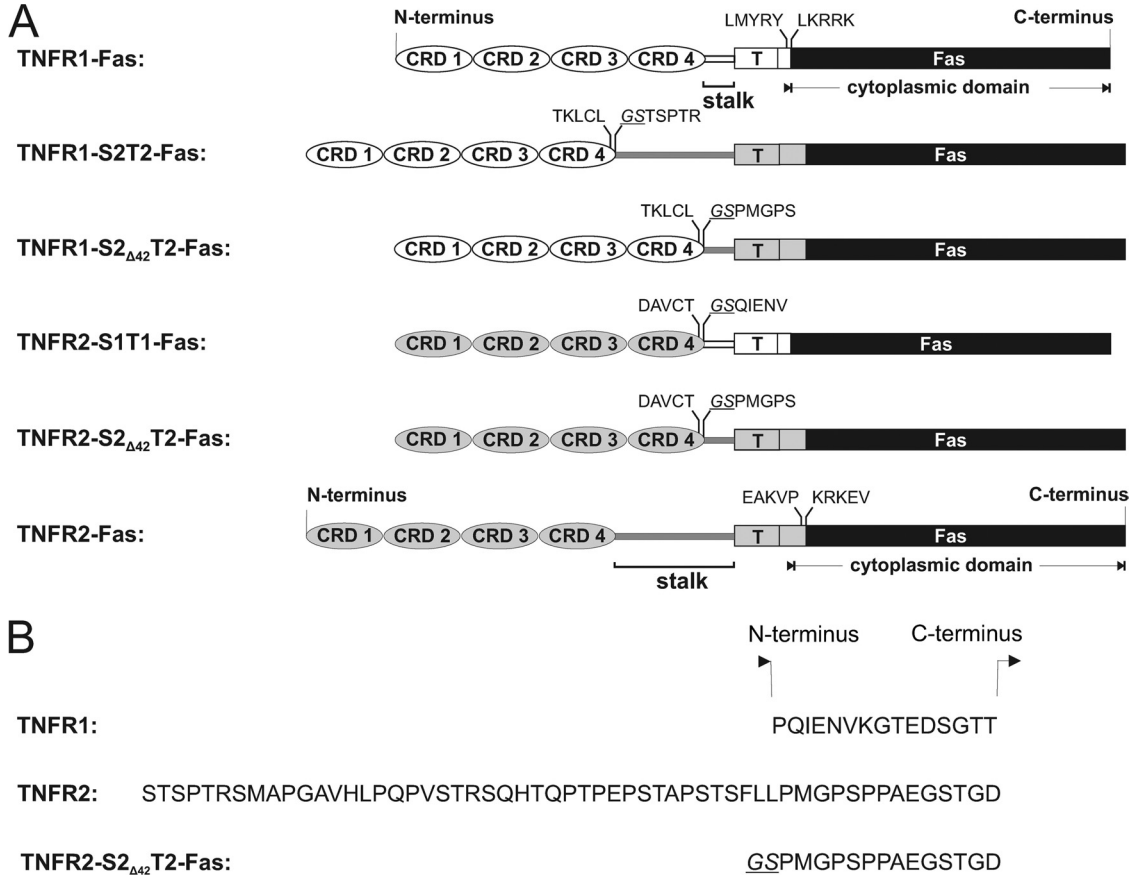

FIG 1 (A) Schematic representation of wild-type TNFR and TNFR-Fas chimeras. The chimeric receptors TNFR1-Fas and TNFR2-Fas consist of the extracellular and transmembrane domains of TNFR1 (aa 1 to 236) and TNFR2 (aa 1 to 301), respectively, and the intracellular domain of Fas (aa 191 to 335). The characteristic four cysteine-rich domains (CRD1 to -4), the stalk region (S), the transmembrane region (T), and the amino acids in the fused regions are indicated. In the TNFR1-S2T2-Fas and TNFR2-S1T1-Fas chimeras, aa 197 to 236 of TNFR1 and aa 202 to 301 of TNFR2 have been exchanged between the chimeric receptors. TNFR1-$S2_{\Delta42}$T2-Fas and TNFR2-$S2_{\Delta42}$T2-Fas represent chimeras in which aa 202 to 243 of the stalk region of TNFR2 have been deleted. (B) Amino acid sequences of the TNFR1 stalk region (aa 197 to 211), the TNFR2 stalk region (aa 202 to 257), and the stalk region in TNFR2-$S_{\Delta42}$T2-Fas after deletion of 42 aa. Underlining indicates additional amino acids introduced through the applied cloning strategy (see the supplemental material).

TNFR2-Fas was resistant to sTNF even at high concentrations (100 ng/ml) (Fig. 2B) (38).

Interestingly, swapping the stalk regions (S) (amino acids [aa] 197 to 211 of TNFR1 and aa 202 to 357 of TNFR2), together with the transmembrane domains (T) between TNFR1-Fas and TNFR2-Fas (TNFR1-S2T2-Fas and TNFR2-S1T1-Fas, respectively), exchanged their sTNF responses almost completely (Fig. 2C and D). TNFR1-S2T2-Fas was fully resistant to sTNF, whereas TNFR2-S1T1-Fas was nearly as susceptible to sTNF as TNFR1-Fas, indicating that the stalk and/or transmembrane region is a critical determinant of sTNF responsiveness. To further determine the influence of the stalk regions of TNFR on the control of sTNF responsiveness, we deleted 42 amino acids in the TNFR2 stalk region of sTNF-unresponsive receptor chimeras, resulting in TNFR1-$S2_{\Delta42}$T2-Fas and TNFR2-$S2_{\Delta42}$T2-Fas (Fig. 1). Notably, sTNF responsiveness was largely restored in both molecules compared to TNFR1-S2T2-Fas and TNFR2-Fas, both containing the full-length TNFR2 stalk region (Fig. 2E and F). While in comparison to CysTNF, TNFR1-$S2_{\Delta42}$T2-Fas showed full sTNF responsiveness, the sTNF sensitivity of TNFR2-$S2_{\Delta42}$T2-Fas was increased by at least 100-fold relative to that of TNFR2-Fas (Fig. 2E and compare Fig. 2F and B, respectively) (38), suggesting that a major determinant of sTNF responsiveness is represented by the stalk regions of the two TNFRs. Flow cytometry analyses performed in parallel with the biofunctional analyses revealed similar chimeric cell surface expression levels, allowing us to exclude the possibility that the differences in sTNF responsiveness are caused simply by differences in cell surface receptor numbers (see Fig. S1 in the supplemental material). To further confirm the role of the TNFR stalk region in controlling sTNF responsiveness, we generated TNFR-Fas chimeras with exchanged transmembrane regions, TNFR2-T1-Fas and TNFR1-T2-Fas. The resulting transmembrane exchange variants showed only minor effects on sTNF responsiveness: the sensitivity increased by approximately a factor of 3 in TNFR2-T1-Fas, and a minor decrease was observed in TNFR1-T2-Fas (see Fig. S3A to H in the supplemental material). Thus, sTNF responsiveness is primarily determined by the stalk regions of the TNFR and to a minor extent by the transmembrane regions.

sTNF-induced downstream signaling of wild-type TNFR2 is abrogated by its stalk region. To verify our results for wild-type receptors, we analyzed the impact of variations in the stalk region of TNFR2 on downstream signaling. Using HeLa cells stably expressing TNFR2, we have shown previously that the differential

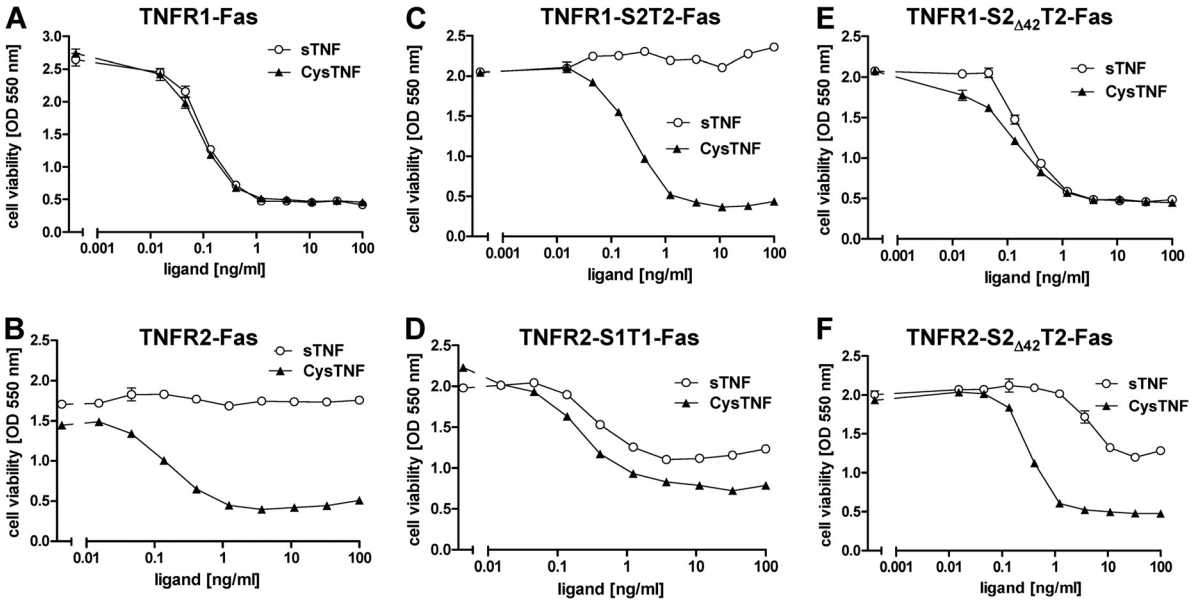

FIG 2 The TNFR2 stalk region inhibits TNFR-Fas responsiveness to sTNF. MF generated from tnfr1$^{-/-}$ tnfr2$^{-/-}$ double-knockout mice were stably transfected with TNFR1-Fas (A), TNFR2-Fas (B), TNFR1-S2T2-Fas (C), TNFR2-S1T1-Fas (D), TNFR1-S2$_{\Delta 42}$T2-Fas (E), and TNFR2-S2$_{\Delta 42}$T2-Fas (F) expression constructs. Cells remained untreated or were treated with sTNF and CysTNF (0.015 to 100 ng/ml each). Cell viability was assessed by crystal violet staining. The means and standard deviations of three replicates are shown. The data are representative of more than four independent experiments.

responsiveness of TNFR2 to sTNF and mTNF is manifested at the level of TRAF2 recruitment (38). We therefore generated HeLa cell lines stably expressing TNFR2, TNFR2-S1T1-R2, or TNFR2-S2$_{\Delta 42}$T2-R2 and analyzed endogenous TRAF2 recruitment by coimmunoprecipitation of the corresponding signaling complexes. While CysTNF-mediated levels of recruitment of TRAF2 were comparable between TNFR2, TNFR2-S1T1-R2, and TNFR2-S2$_{\Delta 42}$T2-R2 (Fig. 3A), we observed significant differences in the sTNF-treated group. In accordance with published data (38), wild-type TNFR2 was not capable of recruiting high levels of TRAF2. In contrast, TNFR2-S1T1-R2 and TNFR2-S2$_{\Delta 42}$T2-R2 both showed enhanced TRAF2 recruitment (Fig. 3B). Parental HeLa cells express low levels of endogenous TNFR1, which is activated by both sTNF and CysTNF and also recruits TRAF2 into its signaling complex. Therefore, to exclude the possibility that TNFR1 stimulation affects TRAF2 recruitment to TNFR2, we repeated coimmunoprecipitation experiments with HeLa TNFR2 and HeLa TNFR2-S2$_{\Delta 42}$T2-Fas cell lines in which TNFR1 expression had been downregulated by RNA interference. These experiments revealed results very similar to those presented in Fig. 3. Again, the partial deletion of the stalk region in TNFR2 relieved the inhibition of sTNF-mediated TRAF2 recruitment (see Fig. S4 in the supplemental material). To assess whether enhanced sTNF-mediated TRAF2 recruitment is followed by upregulated downstream signaling, we explored the nuclear translocation of NF-κB p65 by immunostaining. In order to rule out any p65 activation by endogenously expressed TNFR1, we used our TNFR background-free MF system stably expressing TNFR2, TNFR2-S1T1-R2, or TNFR2-S2$_{\Delta 42}$T2-R2. All three cell lines showed comparably low nuclear p65 background levels of approximately 10.3% ± 1.2% positive cells (Fig. 4A, D, G, and J). Treatment of cells with sTNF for 30 min resulted in an insignificant increase of nuclear p65 for MF TNFR2 (24.0% ± 7.8% positive cells) (compare Fig. 4A, B, and J). Treatment with CysTNF, however, induced nuclear translocation of p65 in a significant proportion of TNFR2-positive MF (45% ± 5%) (Fig. 4B and J). In contrast, significantly different responses could not be observed in MF TNFR2-S1T1-R2 and MF TNFR2-S2$_{\Delta 42}$T2-R2. Both, sTNF and CysTNF treatment caused p65 translocation in more than 45% of cells, similar to CysTNF-treated MF TNFR2 (compare Fig. 4E, F, H, and I with C and J). These findings demonstrate that the stalk region of TNFR2 prevents sTNF responsiveness, whereas CysTNF can overcome this block, probably by avidity effects, mimicking the effects of the physiological stimulus of mTNF.

O-glycosylation and the length of the stalk or particular short amino acid stretches within the stalk do not control sTNF responsiveness. The crucial role of the stalk regions in sTNF responsiveness raises the question of underlying molecular mechanisms. Obvious differences between the stalk regions of TNFR1 and TNFR2 are their overall sequences, their lengths, and their potential glycosylation status. The stalk of TNFR2 is longer (56 aa) than that of TNFR1 (15 aa) and is rich in proline (Pro) residues (Fig. 1B). The stalk region of TNFR2, but not TNFR1, is also highly O-glycosylated (53). To eliminate potential O-glycosylation sites in the stalk region of TNFR2-Fas chimeras, we sequentially mutated Ser and Thr residues of potential O-glycosylation clusters to primarily Ala by site-directed mutagenesis (see Fig. S5A in the supplemental material). Together with this, we functionally analyzed 10 out of 16 different potential O-glycosylation sites (16 was the number of sites predicted using two independent algorithms [see Fig. S5A in the supplemental material]). Although we confirmed that the respective point mutations affected glycosylation of the stalk region (see Fig. S5B in the supplemental material), we could not detect significant effects on sTNF responsiveness (see Fig. S5E and F in the supplemental material). Additionally, we used benzyl-2-acetamido-2-deoxy-α-D-galactopyranoside (Benz-α-GalNAc) as an inhibitor of core 1- and 2-linked mucin-type O-glycosylation. However, despite reduced O-glycosylation and

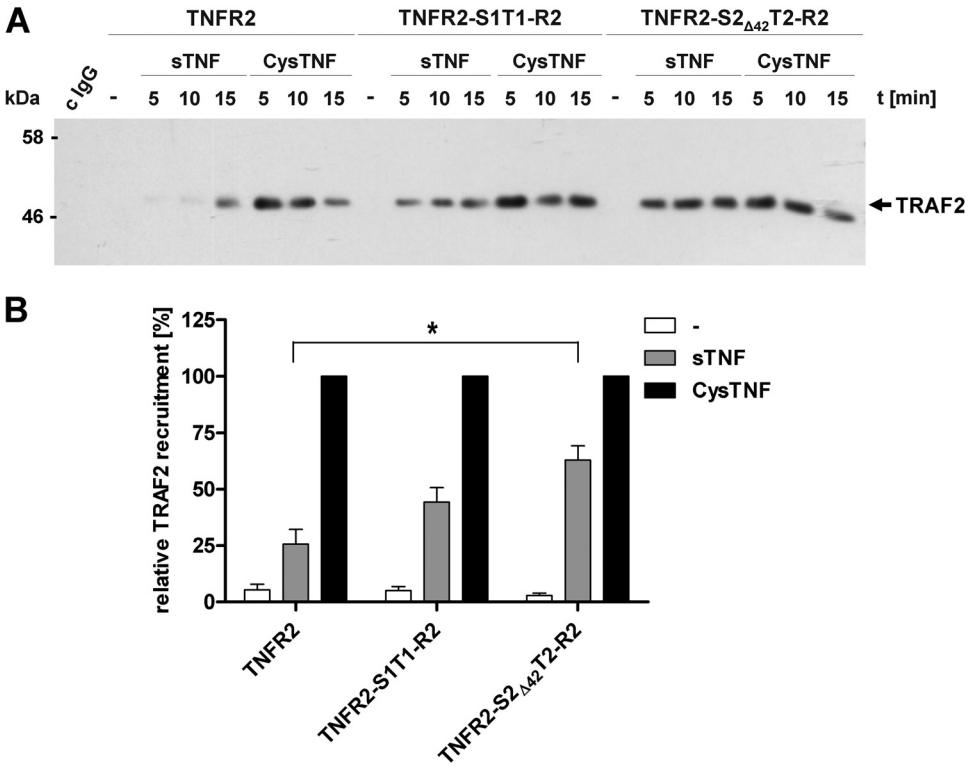

FIG 3 The stalk region prevents sTNF-mediated signaling complex formation of wild-type TNFR2. HeLa cells stably expressing TNFR2, TNFR2-S1T1-R2, and TNFR2-S2$_{\Delta 42}$T2-R2 remained untreated (−) or were treated with sTNF or CysTNF (10 ng/ml each) for 5, 10, and 15 min at 37°C. TNFR signaling complexes were immunoprecipitated and analyzed for TRAF2. cIgG, goat anti-TNFR2 (2 μg). The data shown are representative of at least three independent experiments. (A) TRAF2 Western blot analysis. (B) Quantification of TRAF2 Western blots. TRAF2 levels are expressed as percentages of relative recruitment after 5 min of CysTNF stimulation. The values have been corrected for protein loading as determined from β-actin levels in supernatants after immunoprecipitation. Standard deviations determined from at least three independent experiments are indicated. Statistical differences between samples were assessed by the nonparametric Mann-Whitney U test. *, $P \leq 0.05$.

very similar cell surface expression levels after Benz-α-GalNAc treatment (see Fig. S6A, B, C, F, and G in the supplemental material), no enhanced sTNF responsiveness of TNFR2-Fas was observed (see Fig. S6D, E, H, and I in the supplemental material), indicating that O-glycosylation is unlikely to play a role in the regulation of sTNF responsiveness. Furthermore, replacement of overlapping stretches of 18 to 22 aa with Gly-Ser linkers (Fig. 5A) had no effect on sTNF responsiveness, demonstrating that exchanging approximately a third of the stalk region at any position is not sufficient to overcome sTNF unresponsiveness and that no particular subregion of 10 aa or smaller exists within the relevant 42 aa of the stalk that is responsible for this particular phenotype (Fig. 5B). Sufficient cell surface receptor expression was controlled for by fluorescence-activated cell sorter (FACS) analyses (see Fig. S7 in the supplemental material). However, when the complete stalk regions of TNFR1-Fas and TNFR2-Fas chimeras were replaced with flexible artificial Gly-Ser linkers of 56 aa, high sTNF responsiveness, comparable to that of TNFR1-Fas or the stalk region deletion mutant TNFR2-S2$_{\Delta 42}$T2-Fas, could be observed (Fig. 5C and D). These experiments clearly demonstrate that (i) stalk length, which differs between TNFR1 and TNFR2 by 41 aa (Fig. 1B), is not an important determinant for sTNF responsiveness and (ii) the particular arrangement of amino acids within the TNFR2 stalk as a whole prevents sTNF responsiveness. Therefore, our data suggest that it is the overall conformation and/or orientation of the TNFR2 stalk region, which is, among others, manifested by the Pro-rich sequences, that inhibits sTNF responsiveness of the receptor. This unfavorable arrangement can only be overcome by deletion of the majority of the stalk region or its complete replacement (Fig. 2E and F and 5D). Even high-level expression of TNFR2 is not sufficient to enforce an arrangement required for sTNF responsiveness (see below).

Neither the dissociation constant nor ligand-receptor complex stability correlates with sTNF responsiveness. Most members of the TNFR superfamily contain several cysteine-rich domains (CRD) in their extracellular parts (41) (Fig. 1A). Crystal structure analyses have revealed CRD2 and CRD3 of soluble TNFR1 (5) and TNFR2 (45) as ligand interaction sites, giving no indication of any involvement of the stalk regions. Nevertheless, the stalk regions of the various receptor chimeras could indirectly affect ligand-receptor interaction. To exclude major differences in ligand binding affinities, we performed equilibrium binding studies on ice using radioactively labeled sTNF. Dissociation constant (K_D) values for all receptor chimeras were determined in the range between 20 and 100 pM, indicating that all receptors are occupied by their ligands to more than 95% at the highest sTNF concentration (100 ng/ml) used in our cytotoxicity assays (Table 1; see Fig. S8 in the supplemental material). This provides strong evidence that differences in sTNF binding affinities are not responsible for

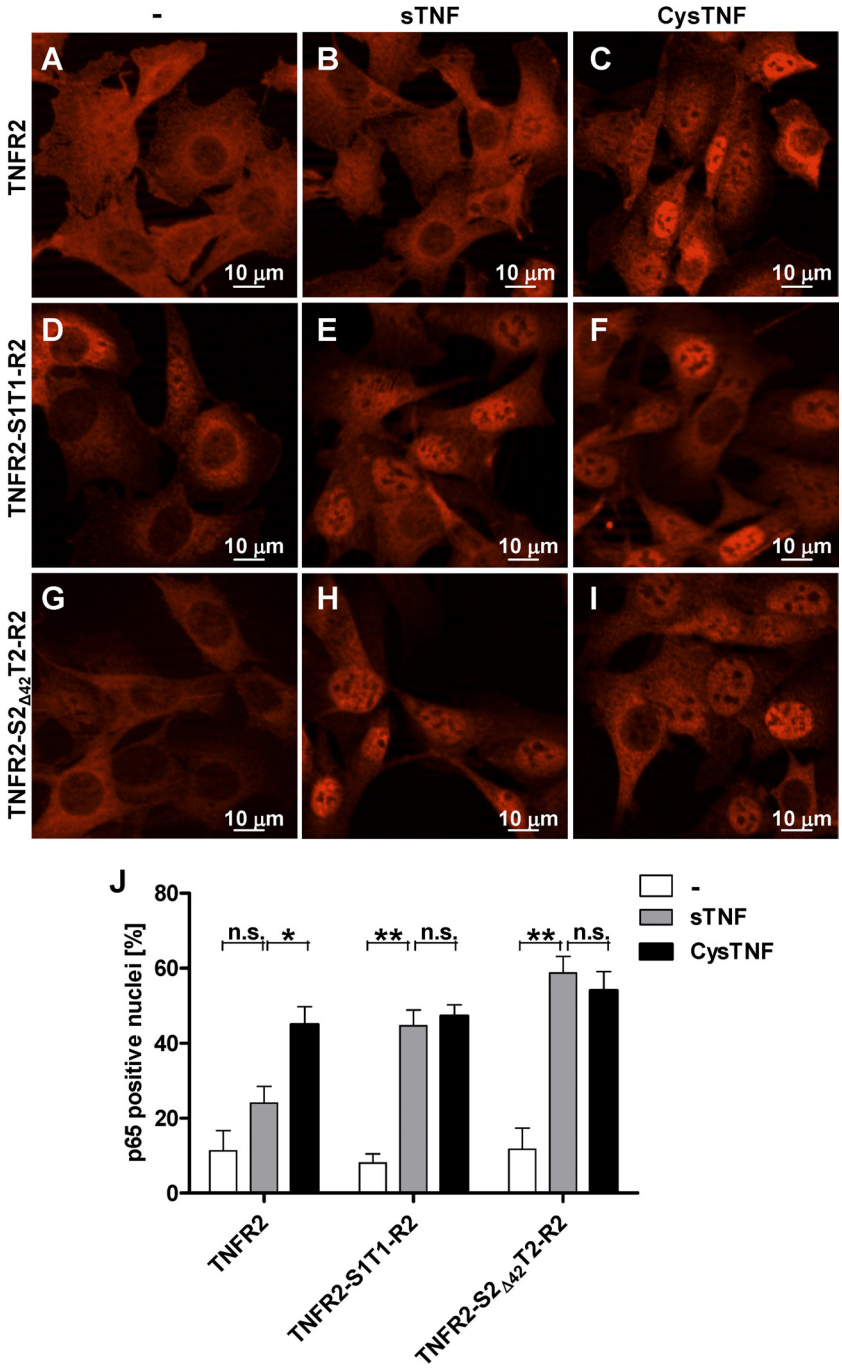

FIG 4 The stalk region determines sTNF-mediated downstream signaling of wild-type TNFR2. MF stably expressing TNFR2 (A to C and J), TNFR2-S1T1-R2 (D to F and J), and TNFR2-S2$_{\Delta 42}$T2-R2 (G to I and J) were left untreated (−) or treated with 100 ng/ml of sTNF or CysTNF. Cells were stained for endogenous p65 and analyzed by fluorescence microscopy. (A to I) Representative images of three independent experiments. (J) Quantification of p65 nucleus-positive cells. The percentages represent proportions of p65 nucleus-positive cells. The standard deviations were calculated from three independent experiments; more than 200 cells/experiment were assessed. Relevant pairs were assessed for their significance by unpaired Student *t* tests (n.s., not significant; *, $P \leq 0.05$; **, $P \leq 0.01$).

the different sTNF responses observed for the diverse TNFR-Fas variants.

Signal initiation at the level of ligand-receptor interaction may be controlled in a more complex manner than by mere overall affinity. We previously observed a strong correlation between sTNF responsiveness and receptor-ligand complex stability at 37°C for both wild-type TNFR and TNFR-Fas chimeras (24, 38). To test the hypothesis that complex stability would inhibit efficient sTNF-receptor signal complex formation, we determined the half-lives ($t_{1/2}$) from dissociation studies of radioactively labeled sTNF at 37°C complexed with TNFR1-S2T2-Fas, TNFR2-S1T1-Fas, and the respective parental TNFR-Fas chimeras. The half-lives of sTNF/TNFR1-Fas and sTNF/TNFR2-Fas that were determined were in good agreement with previous results ($t_{1/2}$ =

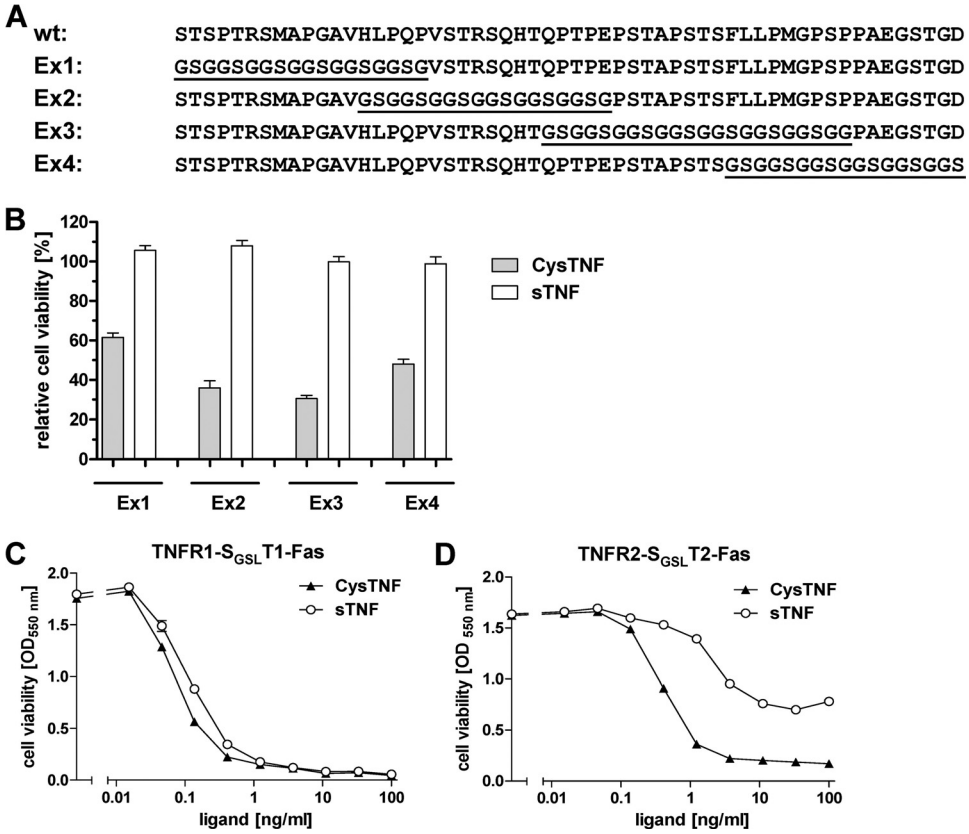

FIG 5 A Gly-Ser stalk region renders TNFR2 responsive to sTNF. (A) Amino acid sequences of the stalk regions of wild-type (wt) TNFR2 and various TNFR2-Fas chimeras in which overlapping amino acid sequences had been replaced by Gly-Ser linkers (Ex1, aa 202 to 219; Ex2, aa 215 to 232; Ex3, aa 228 to 249; Ex4, aa 241 to 257). Linker sequences are underlined. (B to D) MF stably expressing the TNFR2-Fas stalk variants (Ex1, Ex2, Ex3, and Ex4) or TNFR-Fas chimeras in which the complete stalk regions had been replaced by a 56-aa Gly-Ser linker (C and D) were left untreated or treated with sTNF and CysTNF (0.015 to 100 ng/ml). The data shown are representative of at least three independent experiments. (B) Cell viability at 100 ng/ml is expressed as a percentage relative to the viability of untreated cells. The error bars indicate standard deviations from three independent experiments.

30.2 ± 5.5 min and 1.0 ± 0.14 min, respectively) (Fig. 6A and B). However, for the diverse receptor chimeras, no correlation between the ligand-receptor complex half-life and sTNF responsiveness could be observed. Although sTNF-TNFR1-S2T2-Fas complexes were much more stable ($t_{1/2}$ = 7.6 ± 0.9 min) (Fig. 6C) than sTNF-TNFR2-Fas complexes ($t_{1/2}$ = 1.0 ± 0.14 min) (Fig. 6D), TNFR1-S2T2-Fas was incapable of signaling upon sTNF binding (Fig. 2C). Moreover, sTNF-TNFR2-S1T1-Fas exhibited a half-life of 1.8 ± 0.1 min (Fig. 6D). Which was comparable to that of TNFR2-Fas (Fig. 6B) but was highly responsive to sTNF, demonstrating that ligand-receptor complexes with half-lives of only 2 min are capable of inducing downstream signaling (Fig. 2D). In summary, these results demonstrate that the stability of ligand-receptor complexes may contribute to, but clearly does not exclusively determine, sTNF responsiveness.

TABLE 1 Comparison of dissociation constants and sTNF-induced cytotoxicities for different TNF receptor mutants[a]

Mutant	K_D (pM)	Receptor occupancy at 100 ng/ml (%)[b]	Cytotoxicity at 100 ng/ml of sTNF (%)
TNFR1-Fas	93 ± 35	95.6	100
TNFR2-Fas	34 ± 19	98.1	0
TNFR1-S2T2-Fas	46 ± 9	97.8	0
TNFR2-S1T1-Fas	19 ± 9	99.2	62
TNFR1-S2Δ42T2-Fas	59 ± 13	97.1	100
TNFR2-S2Δ42T2-Fas	30 ± 12	98.5	53

[a] Mean values and standard deviations of at least three independent experiments are shown.

[b] The degrees of receptor occupancy at 100 ng/ml sTNF, expressed as percentages, were calculated from the K_D values by applying the following equation: receptor saturation (%) = $c/(c + K_D) \times 100$, with c being the sTNF concentration of interest.

The stalk region of TNFR2 inhibits ligand-independent homotypic receptor dimerization. Homotypic TNFR oligomerization in the absence of ligand has been shown to be important for signal initiation of TNFR and CD95/Fas (13, 68). Our previous experiments suggested that the ability of TNFR1 to form ligand-independent homomultimers is stronger than that of TNFR2 (7). We therefore hypothesized that a higher degree of PLAD-mediated association of receptors could account for increased responsiveness to sTNF and that the stalk region in TNFR may impact homotypic receptor homomultimerization. To assess the degree of homotypic TNFR multimer formation, we used increasing concentrations of the membrane-impermeable chemical cross-linker BS^3. Western blot analysis detected efficient homotypic receptor interaction of TNFR2-S1T1-Fas and TNFR2-S2$_{\Delta 42}$T2-Fas, as indicated by cross-linked homodimers, but not TNFR2-Fas, for which covalently linked receptor dimers were hardly detectable

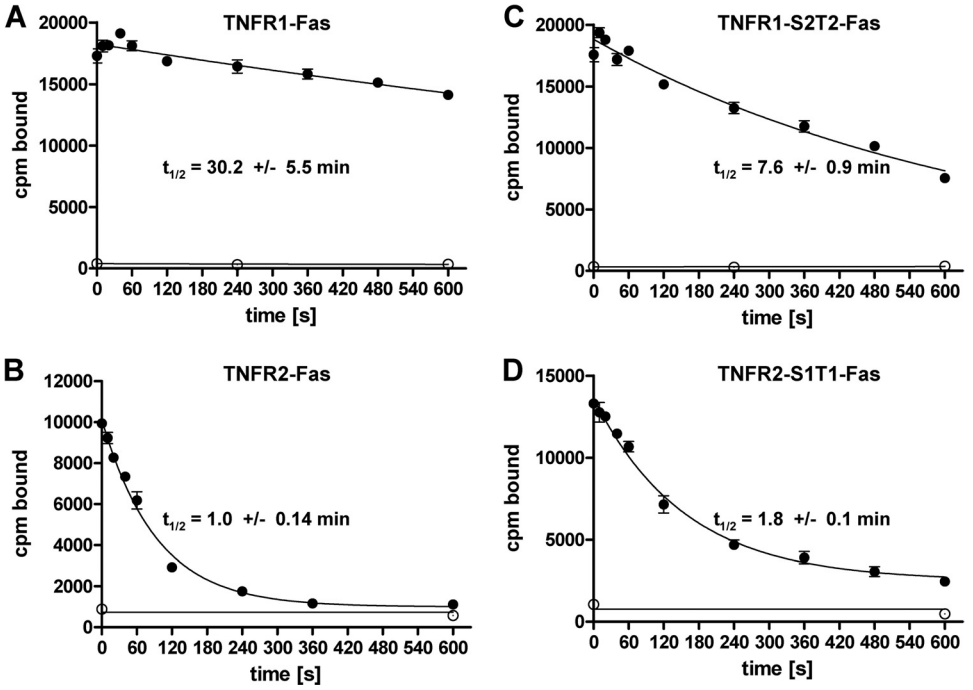

FIG 6 TNF dissociation kinetics at 37°C. MF stably expressing TNFR1-Fas (A), TNFR2-Fas (B), TNFR1-S2T2-Fas (C), and TNFR2-S1T1-Fas (D) were incubated with ^{125}I-labeled TNF at 4°C. Dissociation of ^{125}I-labeled TNF was measured at 37°C in the presence of unlabeled sTNF. Nonspecific binding was determined in the presence of a 200-fold excess of unlabeled sTNF (less than 5% of the total binding) and was subtracted. TNFR complex half-lives were calculated from the one-phase exponential decay curves. The data shown are representative of at least three independent experiments.

(Fig. 7B and D). Importantly, all TNFR2-Fas variants showed very similar cell surface expression levels compared to those of TNFR2-Fas in flow cytometry experiments, indicating that different cross-linking efficiencies were not caused by unequal cell surface expression levels of the various TNFR2-Fas variants (MnX of TNFR2-S1T1-Fas, 15, versus MnX of TNFR2-Fas, 14; MnX of TNFR2-S2$_{\Delta 42}$T2-Fas, 296, versus MnX of TNFR2-Fas, 282) (Fig. 7A and C). These data suggest that the stalk region of TNFR1 facilitates orientation of receptors with high reactivity to the cross-linker, whereas the stalk region of TNFR2 hampers this process. In

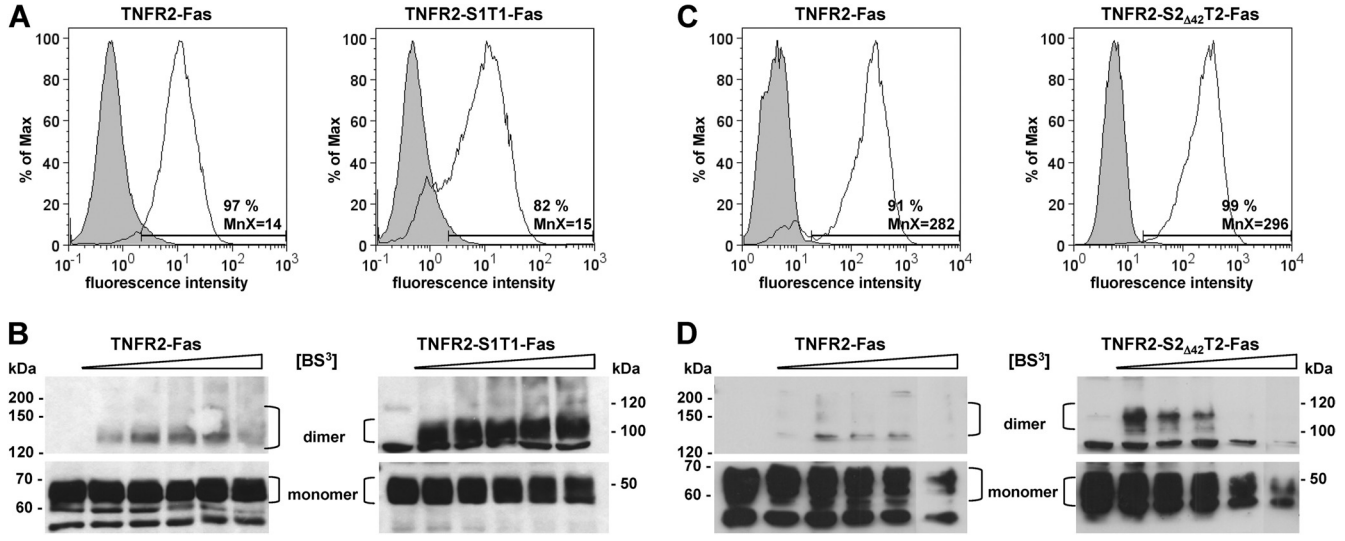

FIG 7 The TNFR2 stalk region prevents homotypic ligand-independent receptor interactions. MF stably expressing TNFR2-Fas, TNFR2-S1T1-Fas, and TNFR2-S2$_{\Delta 42}$T2-Fas were analyzed by flow cytometry (A and C) (anti-TNFR2, black line; secondary antibodies only, gray shaded; percentages, cells gated positive for the chimeras), and homotypic receptor interactions were assessed in chemical cross-linking studies (B and D). (B and D) Cells were incubated with or without the membrane-impermeable chemical cross-linker BS^3 (33 μM to 500 μM). The two images in each panel refer to a single gel each. In order to obtain identical sample sequences, the gel image in panel D was rearranged. Monomeric and dimeric receptor species are indicated. The data shown are representative of three independent experiments.

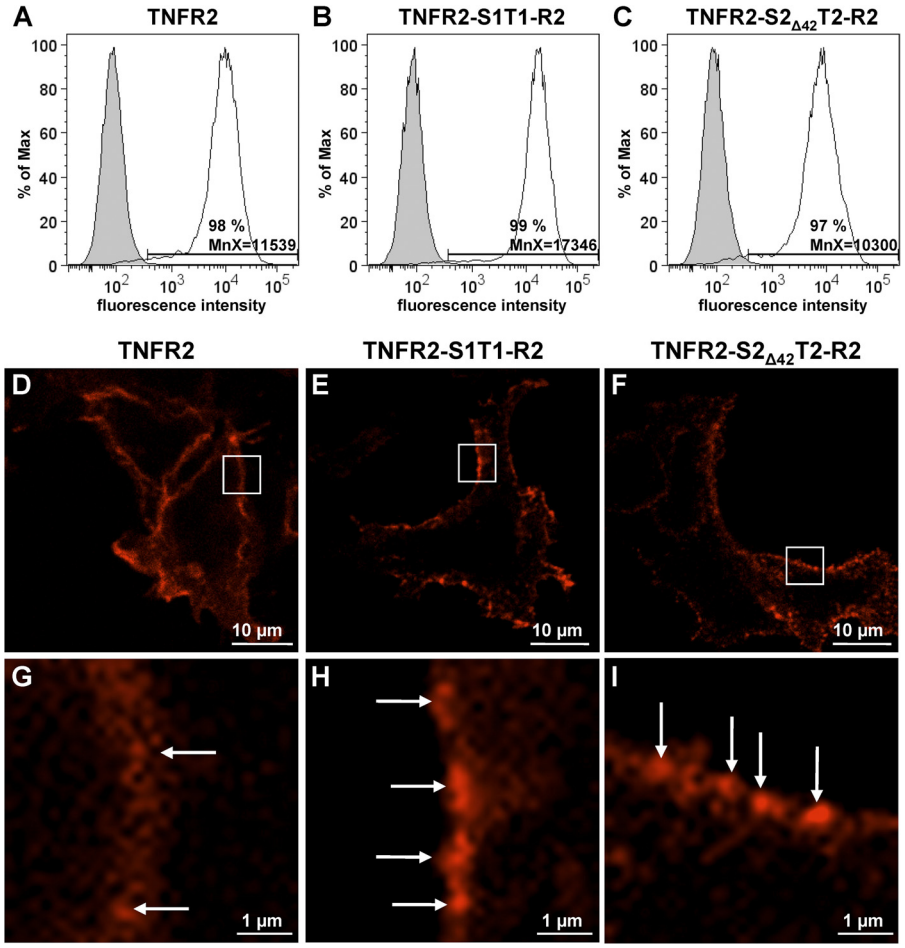

FIG 8 Higher-order receptor cluster formation of wild-type TNFR2 is prevented by the stalk region. HEK 293 Flp-In T-Rex cells inducibly expressing TNFR2 (A, D, and G), TNFR2-S1T1-R2 (B, E, and H), and TNFR2-S2$_{\Delta 42}$T2-R2 (C, F, and I) were left untreated or induced with doxycycline. The data shown are representative of three independent experiments. (A to C) Receptor chimera cell surface expression as analyzed by flow cytometry (anti-TNFR2, black lines; secondary antibodies only, gray shaded; percentages, cells gated positive for the chimeras). (D to I) Higher-order receptor cluster formation. Cells were stained with Alexa Fluor 546-labeled sTNF and analyzed by confocal microscopy. Optical layers from the vertical *z* axis were stacked. The layer images closest to the glass surface of representative cells are shown. The boxes indicate areas that are shown at ×8.4 magnification in panels G, H, and I. Higher-order receptor clusters are indicated by arrows.

support of this hypothesis, the exchange of only the transmembrane domain of TNFR2 with that of TNFR1 (TNFR2-S2T1-Fas) did not significantly affect BS^3-mediated cross-linking product formation and had only minor effects on sTNF responsiveness (see Fig. S3I and E to H in the supplemental material). Together, our data demonstrate that ligand-independent homomultimerization of receptors parallels and possibly favors sTNF responsiveness.

The stalk region of TNFR2 controls receptor cell membrane partitioning to inhibit downstream signaling. The relationship between PLAD-mediated receptor homomultimerization and receptor membrane distribution before ligand binding is unknown. To examine receptor distribution, we used HEK293 Flp-In T-Rex (HEK Flp-In) cells stably expressing wild-type TNFR2 and the respective stalk variants under a doxycycline-inducible promoter. After doxycycline treatment, each of the generated HEK Flp-In cell lines (HEK Flp-In TNFR2, HEK Flp-In TNFR2-S1T1-R2, and HEK Flp-In TNFR2-S2$_{\Delta 42}$T2-R2) showed a homogeneous population of receptor chimera-positive cells at comparable cell surface expression levels (Fig. 8A, B, and C). To visualize the cell surface distribution of these receptors, cells were incubated in parallel on ice with dye-labeled TNF prior to chemical fixation at room temperature and optical analysis by confocal microscopy. By stacking optical layers from the vertical *z* axis, a very homogeneous cell surface distribution for TNFR2 became apparent (Fig. 8D and G). In contrast, TNFR2-S1T1-R2 and TNFR2-S2$_{\Delta 42}$T2-R2 clearly showed nonhomogeneities in their cell surface receptor expression (Fig. 8E, H, F, and I).

Quantitative analyses of the clusters revealed that the cluster size distributions were comparable in all cells investigated irrespective of the type of receptor (chimera) expressed, demonstrating that the most abundant sizes were in the range between 0.36 and 1.08 μm^2 (see Fig. 10A and B). However, 1.9- and 2.7-fold-higher total cluster numbers were observed for TNFR2-S1T1-R2- and TNFR2-S2$_{\Delta 42}$T2-R2-positive cells, respectively, than for TNFR2-expressing cells (see Fig. 10A). Similarly, increases in cluster formation by 2.5- and 2.7-fold for TNFR2-S1T1-Fas and TNFR2-S2$_{\Delta 42}$T2-Fas, respectively, were found in the respective

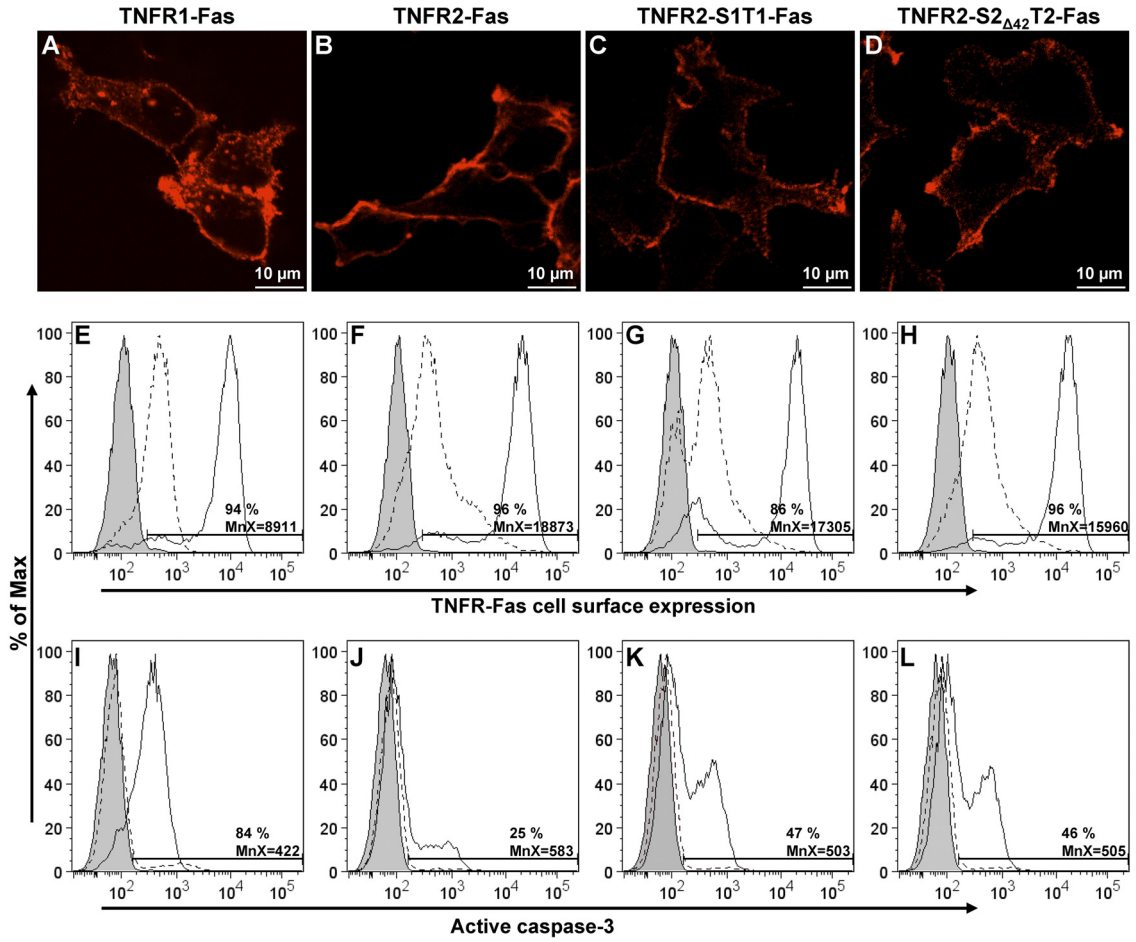

FIG 9 Higher-order receptor cluster formation and activation of TNFR-Fas chimeras are controlled by the stalk region. HEK 293 Flp-In T-Rex cells inducibly expressing TNFR1-Fas (A, E, and I), TNFR2-Fas (B, F, and J), TNFR2-S1T1-Fas (C, G, and K), and TNFR2-S2$_{\Delta 42}$T2-Fas chimeras (D, H, and L) were induced with doxycycline. The data shown are representative of three independent experiments. (A to D) Analyses of the formation of higher-order receptor clusters. Cells grown in the presence of zVAD-fmk were stained on ice using Alexa Fluor 546-labeled sTNF. After fixation, the cells were analyzed by confocal microscopy. (E to H) Analyses of cell surface expression of TNFR-Fas chimeras by flow cytometry. Cells grown in the presence of zVAD-fmk were stained using TNFR1-specific antibodies (black line in panel E) or anti-TNFR2-specific antibodies (black lines in panels F to H). Also shown are unstained cells (gray shaded) and noninduced anti-TNFR-stained cells (dashed lines). (I to L) Analyses of spontaneous caspase 3 activation upon TNFR-Fas chimera overexpression. Cells were stained with anti-active caspase 3 antibodies (black lines) and analyzed by flow cytometry. Also shown are noninduced anti-active caspase 3-stained cells (dashed lines) and induced unstained cells (gray shaded).

TNFR2-Fas-derived cellular systems (see Fig. 10B). These results demonstrate that the competence of TNFR2 to be spontaneously enriched in distinct plasma membrane structures is inhibited by its stalk region.

To address whether ligand-independent local enrichment of TNFRs increases their potential to induce downstream signaling, we performed experiments similar to those described above using HEK Flp-In cells expressing receptor chimeras as cluster sensors. Cell lines stably and inducibly expressing TNFR1-Fas, TNFR2-Fas, TNFR2-S1T1-Fas, and TNFR2-S2$_{\Delta 42}$T2-Fas were generated, and the induction of spontaneous cell death, a well-known phenomenon resulting from higher-level expression of death domain-containing receptors in the absence of the respective ligand (29), was examined. TNFR2-Fas chimeras were homogeneously distributed on the cell surface; in contrast, the stalk variants TNFR2-S1T1-Fas and TNFR2-S2$_{\Delta 42}$T2-Fas were found to be locally enriched after doxycycline induction (Fig. 9B to D and 10B). Importantly, all generated cell lines (HEK Flp-In TNFR2-Fas [Fig. 9F], HEK Flp-In TNFR2-S1T1-Fas [Fig. 9G], and HEK Flp-In TNFR2-S2$_{\Delta 42}$T2-Fas [Fig. 9H]) revealed comparable receptor expression after doxycycline treatment, except that the cell surface expression of TNFR1-Fas was about 2-fold lower (MnX = 8,911) (Fig. 9E). In agreement with our recent studies (9), spontaneous apoptosis was observed in HEK Flp-In TNFR1-Fas cells (Fig. 9I). In contrast, high levels of TNFR2-Fas were well tolerated by the cells, and no pronounced apoptosis induction could be observed, either microscopically by the investigation of the detachment of the cells or in a flow cytometry-based caspase 3 activity assay (Fig. 9I and J). Similar to TNFR1-Fas, the doxycycline-induced expression of TNFR2-S1T1-Fas and TNFR2-S2$_{\Delta 42}$T2-Fas mediated the detachment of the cells, which was paralleled by activation of caspase 3 in nearly half of the cells (Fig. 9K and L). As expected, only TNFR1-Fas was more efficient in the activation of caspase 3 in >80% of the cells (Fig. 9I). These experiments demonstrate that the formation of areas with locally enriched receptors is paralleled by TNFR's potential to induce efficient ligand-

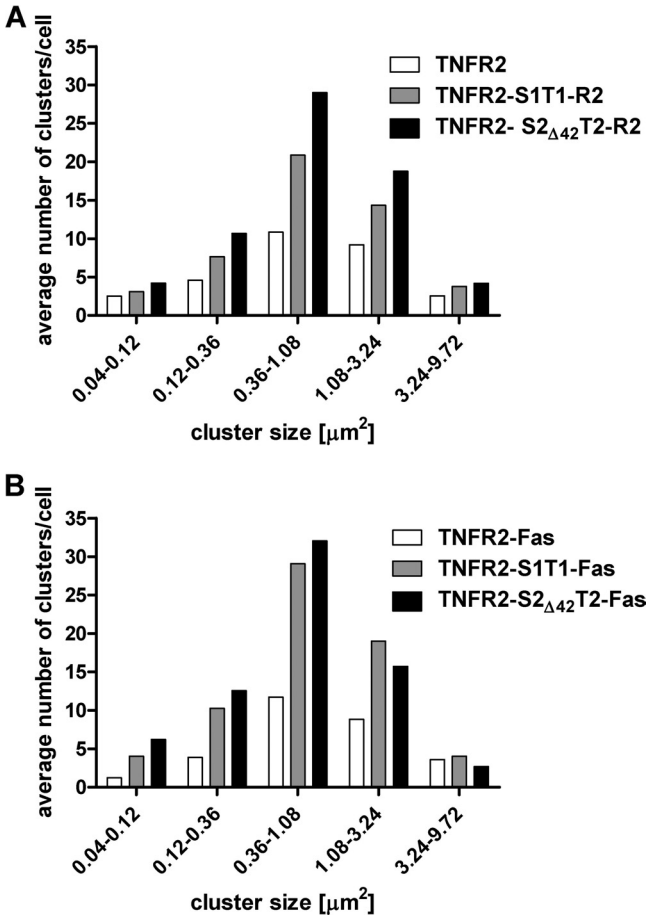

FIG 10 Quantitative analysis of TNFR clusters and distribution of TNFR cluster sizes. Confocal images obtained from the experiments shown in Fig. 8 and 9 (HEK 293 Flp-In T-Rex cells inducibly expressing TNFR2, TNFR2-S1T1-R2, and TNFR2-S2$_{\Delta 42}$T2-R2 [A] and TNFR2-Fas, TNFR2-S1T1-Fas, and TNFR2-S2$_{\Delta 42}$T2-Fas [B] chimeras) were quantified for cluster size distribution (0.04 to 9.72 μm^2) per cell. The data are representative of 36 to 57 cells (A) and 25 to 57 cells (B).

independent downstream signaling. Both the distribution and efficient downstream signaling are controlled by the stalk region, as it antagonizes nonhomogeneous receptor distribution, as well as spontaneous signaling initiation within TNFR2. Thus, sTNF responsiveness requires particular partitioning of the TNF receptors in the plasma membrane, which is controlled by their stalk regions and accompanied by increased homotypic pre-ligand receptor associations.

DISCUSSION

A key property of TNFRs that determines the overall cellular response to TNF is their differential responsiveness to sTNF and mTNF (24, 77). Accordingly, sTNF and mTNF can exert specific and counteracting functions under normal and pathological conditions (36, 64), and distinct TNFR-mediated signaling pathways balance specific immune responses and neurobiological functions (4, 6, 11, 43, 51, 72, 74). Despite the central roles of TNFRs in the regulation of TNF responses, the underlying molecular mechanisms determining receptor responsiveness have long remained unresolved. By using our previously developed unique cellular system and novel TNF variants (10, 38), we identified 42 aa within the stalk region of TNFR2 that, in contrast to the stalk region of TNFR1, effectively prevent responsiveness (Fig. 2, 3, and 4). An assessment of various coparameters for their impacts on sTNF responsiveness revealed that neither ligand-receptor complex stability, which was previously suggested to be a major determinant of sTNF signaling initiation (24, 38), nor O-glycosylation controls sTNF responsiveness (Fig. 6; see Fig. S4 and S5 in the supplemental material). O-glycoslylation is a prominent molecular feature of the TNFR2 stalk region, but not of TNFR1, and might be expected to influence sTNF responsiveness in a manner similar to that seen in other signaling systems (35, 57, 58, 75, 80). However, by using Benzyl-α-GalNAc, as well as a site-directed mutagenesis approach, to eliminate potential glycosylation sites, we could not define a specific role for O-glycosylation in the regulation of sTNF responsiveness (see Fig. S5 and S6 in the supplemental material). After excluding stalk length and any stretch of 10 aa on its own as a determinant of sTNF responsiveness (Fig. 5), our data together suggest that a likely determinant controlling the receptor's unresponsiveness to sTNF is TNFR2 stalk rigidity, which is attributable to its richness in proline residues. In this context, it is salient to note that longer, Pro-rich stalk regions are characteristic of other members of the TNFR superfamily, including Ox40, CD27, 4-1BB, and TACI. These receptors require preoligomerized soluble ligands for efficient activation (8, 42, 46, 79), suggesting that, like TNFR2, the respective membrane-bound ligands are in fact their relevant activators. Moreover, differential responsiveness to soluble and membrane-bound ligand has been described for DR5, but not DR4 (76), and it is noteworthy that the stalk region of DR5 (but not of DR4) is comparable in length and proline content to the TNFR2 stalk region.

Another molecular feature with potential relevance for ligand binding and signal initiation of several TNFR superfamily members, including TNFR1, TNFR2, and Fas, is the PLAD located in the N-terminal CRD1 of the receptors. This domain mediates homotypic receptor interactions in the absence of ligand and has been proposed to mediate stable ligand-receptor clusters (9, 12, 13, 45, 49, 68). Chan et al. have shown that removal of the PLAD-positive CRD1 abolishes ligand binding (13), although CRD1 of TNFR1 does not appear to be directly involved in ligand-receptor interaction (5, 9). Our own experiments argued for a scaffold function of CRD1 in the stabilization of CRD2 and supported the hypothesis of Chan et al. that chemical cross-linkers preferentially detect PLAD-mediated homomultimers (9). However, data presented here demonstrate that the receptor's ability to allow formation of covalently cross-linked homodimers correlates well with sTNF responsiveness, but not with its ligand binding affinity, arguing against a need for PLAD-mediated avidity effects for high-affinity binding (see Fig. S8 in the supplemental material and Table 1). Our data thus support the notion that PLAD-mediated homotypic receptor preassembly is not mandatory for high-affinity sTNF binding but rather is essential for sTNF signaling initiation by the formation of stable ligand-receptor clusters.

Receptor clustering confers several advantages for signal transduction, including increased sensitivity and specificity, simultaneity of response, and the segregation of similar signaling systems (17). Indeed, ligand-mediated trimerization of TNFR is believed not to be sufficient for signal initiation, but oligomerization of ligand-receptor complexes into larger clusters has been observed in parallel with signaling initiation (9, 19, 21, 28, 38, 39, 60, 67, 69,

71). Membrane-bound ligands themselves tend to be locally enriched and inevitably result in the oligomerization of receptors (27). However, other TNFRs, such as TNFR1 and DR4 (76), can be readily activated by the respective soluble forms of their ligands, which is perhaps surprising given their low cell surface numbers (typically only 300 to 1,000 receptors per cell for TNFR1) (55). Our data from wild-type TNFR2, the TNFR2-Fas chimera, and their stalk variants indicate that the ability to respond to sTNF is favored by ligand-independent local enrichment of receptors in the plasma membrane (compare Fig. 2B, D, and F with 5A to D and 6 with 7 and 8). Moreover, we identified the stalk region as the critical determinant controlling spontaneous local enrichment of wild-type TNFR2, as well as TNFR2-Fas chimeras (Fig. 8D to I and 9A to D). Our experiments indicate that the ability of receptors to become locally enriched in the absence of ligand is essential, both for efficient signal transduction by sTNF and for the induction of spontaneous, ligand-independent cell death (Fig. 9I to L). Parallel to local enrichment, enhanced formation of cross-linker-reactive homodimers was observed. Thus, we propose that cell surface TNFR distribution, regulated by the stalk regions, ultimately controls homotypic receptor preassembly; in turn, the requirement for soluble or membrane-bound ligand is defined, along with the efficiency of subsequent signal initiation.

What might cause TNF receptors to distribute nonhomogeneously in the cellular membrane and to be enriched in locally confined areas? Receptor preassembly/enrichment in transient small (6 to 12 nm in diameter) cholesterol-dependent nanoclusters may provide an explanation and reportedly promotes efficient signal complex formation (26). In support of this, TNFR1, but not TNFR2, contains a potential cholesterol-binding motif in its transmembrane domain (LMYRYQR; aa 232 to 238) (18), which is maintained in TNFR1-Fas, TNFR2-S1T1-Fas, TNFR2-S2T1-Fas, and TNFR2-S1T1-R2 chimeras. Indeed, in contrast to TNFR2, TNFR1 was found to localize to cholesterol- and sphingolipid-enriched membrane microdomains in the plasma membrane (15, 16, 30, 40, 44, 48). Consistent with this, we have observed a much slower membrane diffusion of TNFR1 than of TNFR2 that is sensitive to cholesterol depletion (23). Together, these data suggest that the enrichment of the two TNFRs in different membrane microcompartments might control receptor distribution, PLAD-mediated homomultimerization, and, thus, sTNF responsiveness. However, results from our TNFR2-S2T1-Fas chimera experiments demonstrate that, rather than the transmembrane region, the extracellular stalk region is the key orchestrator of these processes: TNFR2-S2T1-Fas, similar to TNFR2-Fas, does not show pronounced levels of cross-linker-sensitive homodimers, whereas TNFR2-S2$_{\Delta 42}$T2-Fas is efficient in the formation of preassembled receptors (Fig. 7D; see Fig. S3I in the supplemental material). Indeed, TNFR2-S2T1-Fas is largely unresponsive to sTNF (see Fig. S3H in the supplemental material). In addition, stalk-mediated disruption of receptor localization in nanostructured membrane microdomains might represent a mechanism for downregulating sTNF responsiveness. With this in mind, it is worth noting that in the case of Fas, T-cell receptor (TCR) engagement leads to the redistribution of this death receptor into "lipid rafts," rendering T cells sensitive to Fas-specific antibodies in the absence of a secondary cross-linker (47). This rearrangement seems to be regulated by Rac-1-dependent cytoskeletal remodeling, presumably through the dephosphorylation of the ezrin-radixin-moesin (ERM) proteins (52, 59). Due to sequence homologies between Fas and TNFR2 in the membrane-proximal intracellular region, an interaction of TNFR2 with the cytoskeleton is conceivable (63). Alternatively, stalk-mediated conformational hindrance, posttranslational modifications, or lipid-protein interactions could antagonize cluster formation. Due to its comparable interactions with both TNF receptors and its competition with ligand binding, the recently identified TNFR-interacting molecule progranulin does not appear to represent a good candidate for such an interaction partner (73). Overall, the definitive means by which the long, proline-rich stalk region interferes with local enrichment of receptors, resulting in reduced formation of PLAD-mediated homomultimers and sTNF unresponsiveness, remains elusive but highlights another exciting level of complexity of receptor activity regulation.

In conclusion, our data reveal a novel mechanism of TNFR partitioning in the absence of ligand controlling sTNF responsiveness. Our comprehensive analysis identified the stalk regions of TNFR as key determinants for TNFR arrangements and sTNF responsiveness. Complications currently associated with TNF-directed therapeutics, including impaired host defense and the paradoxical triggering of autoimmunity, demand the design of more TNFR-selective therapeutic agents (20, 36, 37). The stalk regions of TNFR may become intriguing targets for the specific modulation of TNFR responses *in vivo*.

ACKNOWLEDGMENTS

We thank K. Jablonski for excellent technical assistance, M. Sweeney for her help with the Andor confocal microscopy, and A. Laude of the bioimaging facility, Newcastle University, for assisting with the live-imaging microscopy and Volocity software. We are grateful to D. Männel for the murine fibroblasts and A. Strasser (The Walter and Eliza Hall Institute, Melbourne, Australia) for pEF PGKpuro, and we thank I.-W. von Broen (Knoll Ag, Ludwigshafen, Germany) for recombinant TNF. We thank A. Pratt and O. Heidenreich for critical reading of the manuscript.

This work was supported by grants from the German Research Foundation (DFG) (KR3307/1-1 and SFB 495). The Andor microscopy system was funded by the Wellcome Trust (087961).

REFERENCES

1. **Alexopoulou L, et al.** 2006. Transmembrane TNF protects mutant mice against intracellular bacterial infections, chronic inflammation and autoimmunity. Eur. J. Immunol. **36**:2768–2780.
2. **Allenbach C, Launois P, Mueller C, Tacchini-Cottier F.** 2008. An essential role for transmembrane TNF in the resolution of the inflammatory lesion induced by Leishmania major infection. Eur. J. Immunol. **38**:720–731.
3. **Apostolaki M, Armaka M, Victoratos P, Kollias G.** 2010. Cellular mechanisms of TNF function in models of inflammation and autoimmunity. Curr. Dir. Autoimmun. **11**:1–26.
4. **Ban L, et al.** 2008. Selective death of autoreactive T cells in human diabetes by TNF or TNF receptor 2 agonism. Proc. Natl. Acad. Sci. U. S. A. **105**:13644–13649.
5. **Banner DW, et al.** 1993. Crystal structure of the soluble human 55 kd TNF receptor-human TNF beta complex: implications for TNF receptor activation. Cell **73**:431–445.
6. **Bluml S, et al.** 2010. Antiinflammatory effects of tumor necrosis factor on hematopoietic cells in a murine model of erosive arthritis. Arthritis Rheum. **62**:1608–1619.
7. **Boschert V, et al.** 2010. Single chain TNF derivatives with individually mutated receptor binding sites reveal differential stoichiometry of ligand receptor complex formation for TNFR1 and TNFR2. Cell Signal **22**:1088–1096.
8. **Bossen C, et al.** 2008. TACI, unlike BAFF-R, is solely activated by oligomeric BAFF and APRIL to support survival of activated B cells and plasmablasts. Blood **111**:1004–1012.

9. **Branschadel M, et al.** 2010. Dual function of cysteine rich domain (CRD) 1 of TNF receptor type 1: conformational stabilization of CRD2 and control of receptor responsiveness. Cell Signal **22**:404–414.
10. **Bryde S, et al.** 2005. Tumor necrosis factor (TNF)-functionalized nanostructured particles for the stimulation of membrane TNF-specific cell responses. Bioconjug. Chem. **16**:1459–1467.
11. **Calzascia T, et al.** 2007. TNF-alpha is critical for antitumor but not antiviral T cell immunity in mice. J. Clin. Invest. **117**:3833–3845.
12. **Chan FK.** 2007. Three is better than one: pre-ligand receptor assembly in the regulation of TNF receptor signaling. Cytokine **37**:101–107.
13. **Chan FK, et al.** 2000. A domain in TNF receptors that mediates ligand-independent receptor assembly and signaling. Science **288**:2351–2354.
14. **Chen X, Oppenheim JJ.** 2011. Contrasting effects of TNF and anti-TNF on the activation of effector T cells and regulatory T cells in autoimmunity. FEBS Lett. **585**:3611–3618.
15. **Cottin V, Doan JE, Riches DW.** 2002. Restricted localization of the TNF receptor CD120a to lipid rafts: a novel role for the death domain. J. Immunol. **168**:4095–4102.
16. **D'Alessio A, et al.** 2010. Targeting of tumor necrosis factor receptor 1 to low density plasma membrane domains in human endothelial cells. J. Biol. Chem. **285**:23868–23879.
17. **Duke T, Graham I.** 2009. Equilibrium mechanisms of receptor clustering. Prog. Biophys. Mol. Biol. **100**:18–24.
18. **Epand RM, Thomas A, Brasseur R, Epand RF.** 2010. Cholesterol interaction with proteins that partition into membrane domains: an overview. Subcell. Biochem. **51**:253–278.
19. **Esposito D, et al.** 2010. Solution NMR investigation of the CD95/FADD homotypic death domain complex suggests lack of engagement of the CD95 C terminus. Structure **18**:1378–1390.
20. **Faustman D, Davis M.** 2010. TNF receptor 2 pathway: drug target for autoimmune diseases. Nat. Rev. Drug Discov. **9**:482–493.
21. **Feig C, Tchikov V, Schutze S, Peter ME.** 2007. Palmitoylation of CD95 facilitates formation of SDS-stable receptor aggregates that initiate apoptosis signaling. EMBO J. **26**:221–231.
22. **Fontaine V, et al.** 2002. Neurodegenerative and neuroprotective effects of tumor necrosis factor (TNF) in retinal ischemia: opposite roles of TNF receptor 1 and TNF receptor 2. J. Neurosci. **22**:RC216.
23. **Gerken M, et al.** 2010. Fluorescence correlation spectroscopy reveals topological segregation of the two tumor necrosis factor membrane receptors. Biochim. Biophys. Acta **1798**:1081–1089.
24. **Grell M, et al.** 1995. The transmembrane form of tumor necrosis factor is the prime activating ligand of the 80 kDa tumor necrosis factor receptor. Cell **83**:793–802.
25. **Grell M, Wajant H, Zimmermann G, Scheurich P.** 1998. The type 1 receptor (CD120a) is the high-affinity receptor for soluble tumor necrosis factor. Proc. Natl. Acad. Sci. U. S. A. **95**:570–575.
26. **Harding AS, Hancock JF.** 2008. Using plasma membrane nanoclusters to build better signaling circuits. Trends Cell Biol. **18**:364–371.
27. **Henkler F, et al.** 2005. The extracellular domains of FasL and Fas are sufficient for the formation of supramolecular FasL-Fas clusters of high stability. J. Cell Biol. **168**:1087–1098.
28. **Holler N, et al.** 2003. Two adjacent trimeric Fas ligands are required for Fas signaling and formation of a death-inducing signaling complex. Mol. Cell. Biol. **23**:1428–1440.
29. **Hsu H, Shu HB, Pan MG, Goeddel DV.** 1996. TRADD-TRAF2 and TRADD-FADD interactions define two distinct TNF receptor 1 signal transduction pathways. Cell **84**:299–308.
30. **Hunter I, Nixon GF.** 2006. Spatial compartmentalization of tumor necrosis factor (TNF) receptor 1-dependent signaling pathways in human airway smooth muscle cells. Lipid rafts are essential for TNF-alpha-mediated activation of RhoA but dispensable for the activation of the NF-kappaB and MAPK pathways. J. Biol. Chem. **281**:34705–34715.
31. **Kim EY, Priatel JJ, Teh SJ, Teh HS.** 2006. TNF receptor type 2 (p75) functions as a costimulator for antigen-driven T cell responses in vivo. J. Immunol. **176**:1026–1035.
32. **Kim EY, Teh HS.** 2004. Critical role of TNF receptor type-2 (p75) as a costimulator for IL-2 induction and T cell survival: a functional link to CD28. J. Immunol. **173**:4500–4509.
33. **Kim EY, Teh HS.** 2001. TNF type 2 receptor (p75) lowers the threshold of T cell activation. J. Immunol. **167**:6812–6820.
34. **Kleijwegt FS, et al.** 2010. Critical role for TNF in the induction of human antigen-specific regulatory T cells by tolerogenic dendritic cells. J. Immunol. **185**:1412–1418.
35. **Klima M, Zajedova J, Doubravska L, Andera L.** 2009. Functional analysis of the posttranslational modifications of the death receptor 6. Biochim. Biophys. Acta **1793**:1579–1587.
36. **Kollias G, Kontoyiannis D.** 2002. Role of TNF/TNFR in autoimmunity: specific TNF receptor blockade may be advantageous to anti-TNF treatments. Cytokine Growth Factor Rev. **13**:315–321.
37. **Kontermann RE, et al.** 2008. A humanized tumor necrosis factor receptor 1 (TNFR1)-specific antagonistic antibody for selective inhibition of tumor necrosis factor (TNF) action. J. Immunother. **31**:225–234.
38. **Krippner-Heidenreich A, et al.** 2002. Control of receptor-induced signaling complex formation by the kinetics of ligand/receptor interaction. J. Biol. Chem. **277**:44155–44163.
39. **Kuhne MR, et al.** 1997. Assembly and regulation of the CD40 receptor complex in human B cells. J. Exp. Med. **186**:337–342.
40. **Legler DF, Micheau O, Doucey MA, Tschopp J, Bron C.** 2003. Recruitment of TNF receptor 1 to lipid rafts is essential for TNFalpha-mediated NF-kappaB activation. Immunity **18**:655–664.
41. **Locksley RM, Killeen N, Lenardo MJ.** 2001. The TNF and TNF receptor superfamilies: integrating mammalian biology. Cell **104**:487–501.
42. **Mackay F, Schneider P.** 2009. Cracking the BAFF code. Nat. Rev. Immunol. **9**:491–502.
43. **Masli S, Turpie B.** 2009. Anti-inflammatory effects of tumour necrosis factor (TNF)-alpha are mediated via TNF-R2 (p75) in tolerogenic transforming growth factor-beta-treated antigen-presenting cells. Immunology **127**:62–72.
44. **Micheau O, Tschopp J.** 2003. Induction of TNF receptor I-mediated apoptosis via two sequential signaling complexes. Cell **114**:181–190.
45. **Mukai Y, et al.** 2010. Solution of the structure of the TNF-TNFR2 complex. Sci. Signal **3**:ra83. doi:10.1126/scisignal.2000954.
46. **Muller N, Wyzgol A, Munkel S, Pfizenmaier K, Wajant H.** 2008. Activity of soluble OX40 ligand is enhanced by oligomerization and cell surface immobilization. FEBS J. **275**:2296–2304.
47. **Muppidi JR, Siegel RM.** 2004. Ligand-independent redistribution of Fas (CD95) into lipid rafts mediates clonotypic T cell death. Nat. Immunol. **5**:182–189.
48. **Muppidi JR, Tschopp J, Siegel RM.** 2004. Life and death decisions: secondary complexes and lipid rafts in TNF receptor family signal transduction. Immunity **21**:461–465.
49. **Naismith JH, Devine TQ, Brandhuber BJ, Sprang SR.** 1995. Crystallographic evidence for dimerization of unliganded tumor necrosis factor receptor. J. Biol. Chem. **270**:13303–13307.
50. **Naude PJ, den Boer JA, Luiten PG, Eisel UL.** 2011. Tumor necrosis factor receptor cross-talk. FEBS J. **278**:888–898.
51. **Nijholt IM, Granic I, Luiten PG, Eisel UL.** 2011. TNFR2: target for therapeutics against neurodegenerative diseases? Adv. Exp. Med. Biol. **691**:567–573.
52. **Parlato S, et al.** 2000. CD95 (APO-1/Fas) linkage to the actin cytoskeleton through ezrin in human T lymphocytes: a novel regulatory mechanism of the CD95 apoptotic pathway. EMBO J. **19**:5123–5134.
53. **Pennica D, et al.** 1993. Biochemical characterization of the extracellular domain of the 75-kilodalton tumor necrosis factor receptor. Biochemistry **32**:3131–3138.
54. **Peschon JJ, et al.** 1998. TNF receptor-deficient mice reveal divergent roles for p55 and p75 in several models of inflammation. J. Immunol. **160**:943–952.
55. **Pfizenmaier K, Kronke M, Scheurich P, Nagel GA.** 1987. Tumor necrosis factor (TNF) alpha: control of TNF-sensitivity and molecular mechanisms of TNF-mediated growth inhibition. Blut **55**:1–10.
56. **Pronk CJ, Veiby OP, Bryder D, Jacobsen SE.** 2011. Tumor necrosis factor restricts hematopoietic stem cell activity in mice: involvement of two distinct receptors. J. Exp. Med. **208**:1563–1570.
57. **Rabinovich GA, Toscano MA.** 2009. Turning 'sweet' on immunity: galectin-glycan interactions in immune tolerance and inflammation. Nat. Rev. Immunol. **9**:338–352.
58. **Rabinovich GA, Toscano MA, Jackson SS, Vasta GR.** 2007. Functions of cell surface galectin-glycoprotein lattices. Curr. Opin. Struct. Biol. **17**:513–520.
59. **Ramaswamy M, et al.** 2007. Cutting edge: Rac GTPases sensitize activated T cells to die via Fas. J. Immunol. **179**:6384–6388.
60. **Ranzinger J, et al.** 2009. Nanoscale arrangement of apoptotic ligands reveals a demand for a minimal lateral distance for efficient death receptor activation. Nano Lett. **9**:4240–4245.
61. **Rauert H, et al.** 2010. Membrane tumor necrosis factor (TNF) induces

p100 processing via TNF receptor-2 (TNFR2). J. Biol. Chem. **285**:7394–7404.
62. **Rezzoug F, et al.** 2008. TNF-alpha is critical to facilitate hemopoietic stem cell engraftment and function. J. Immunol. **180**:49–57.
63. **Ruan W, Lee CT, Desbarats J.** 2008. A novel juxtamembrane domain in tumor necrosis factor receptor superfamily molecules activates Rac1 and controls neurite growth. Mol. Biol. Cell **19**:3192–3202.
64. **Ruuls SR, et al.** 2001. Membrane-bound TNF supports secondary lymphoid organ structure but is subservient to secreted TNF in driving autoimmune inflammation. Immunity **15**:533–543.
65. **Saunders BM, Briscoe H, Britton WJ.** 2004. T cell-derived tumour necrosis factor is essential, but not sufficient, for protection against Mycobacterium tuberculosis infection. Clin. Exp. Immunol. **137**:279–287.
66. **Saunders BM, Britton WJ.** 2007. Life and death in the granuloma: immunopathology of tuberculosis. Immunol. Cell Biol. **85**:103–111.
67. **Schneider-Brachert W, et al.** 2004. Compartmentalization of TNF receptor 1 signaling: internalized TNF receptosomes as death signaling vesicles. Immunity **21**:415–428.
68. **Siegel RM, et al.** 2000. Fas preassociation required for apoptosis signaling and dominant inhibition by pathogenic mutations. Science **288**:2354–2357.
69. **Siegel RM, et al.** 2004. SPOTS: signaling protein oligomeric transduction structures are early mediators of death receptor-induced apoptosis at the plasma membrane. J. Cell Biol. **167**:735–744.
70. **Strand V, Kimberly R, Isaacs JD.** 2007. Biologic therapies in rheumatology: lessons learned, future directions. Nat. Rev. Drug Discov. **6**:75–92.
71. **Swee LK, et al.** 2009. Biological activity of ectodysplasin A is conditioned by its collagen and heparan sulfate proteoglycan-binding domains. J. Biol. Chem. **284**:27567–27576.
72. **Takei Y, Laskey R.** 2008. Interpreting crosstalk between TNF-alpha and NGF: potential implications for disease. Trends Mol. Med. **14**:381–388.
73. **Tang W, et al.** 2011. The growth factor progranulin binds to TNF receptors and is therapeutic against inflammatory arthritis in mice. Science **332**:478–484.
74. **Veroni C, et al.** 2010. Activation of TNF receptor 2 in microglia promotes induction of anti-inflammatory pathways. Mol. Cell Neurosci. **45**:234–244.
75. **Wagner KW, et al.** 2007. Death-receptor O-glycosylation controls tumor-cell sensitivity to the proapoptotic ligand Apo2L/TRAIL. Nat. Med. **13**:1070–1077.
76. **Wajant H, et al.** 2001. Differential activation of TRAIL-R1 and -2 by soluble and membrane TRAIL allows selective surface antigen-directed activation of TRAIL-R2 by a soluble TRAIL derivative. Oncogene **20**:4101–4106.
77. **Wajant H, Pfizenmaier K, Scheurich P.** 2003. Tumor necrosis factor signaling. Cell Death Differ. **10**:45–65.
78. **Winthrop KL.** 2006. Risk and prevention of tuberculosis and other serious opportunistic infections associated with the inhibition of tumor necrosis factor. Nat. Clin. Pract Rheumatol. **2**:602–610.
79. **Wyzgol A, et al.** 2009. Trimer stabilization, oligomerization, and antibody-mediated cell surface immobilization improve the activity of soluble trimers of CD27L, CD40L, 41BBL, and glucocorticoid-induced TNF receptor ligand. J. Immunol. **183**:1851–1861.
80. **Xu Z, Weiss A.** 2002. Negative regulation of CD45 by differential homodimerization of the alternatively spliced isoforms. Nat. Immunol. **3**:764–771.